

Optimization scheme of stereogram synthesis algorithm with wide-activated deep residual network super-resolution for cylindrical grating display

Zheqiang Wang,^a Guanglin Yang^{a,*} and Haiyan Xie^b

^aPeking University, Laboratory of Signal and Information Processing,

Department of Electronics, Beijing, China

^bChina Science Patent Trademark Agents Ltd., Beijing, China

Abstract. An optimization scheme based on wide-activated deep residual network super-resolution (WDSR) is proposed for the stereoscopic image synthesis algorithm of a cylindrical grating display. Unlike the traditional synthesis scheme, the WDSR algorithm is used to replace, partially or fully, the interpolation algorithm to reduce the antialiasing effect of the image. Thereafter, the viewpoint mapping process is accelerated based on the subpixel mapping table by making masks. Subsequently, a stereoscopic image with a better quality is obtained. The experimental results demonstrate that the proposed scheme can improve the signal-to-noise ratio and quality of the stereoscopic composite image when the same subviewpoint image is used for verification. © 2021 Society of Photo-Optical Instrumentation Engineers (SPIE) [DOI: [10.1117/1.OE.60.1113101](https://doi.org/10.1117/1.OE.60.1113101)]

Keywords: naked-eye three-dimensional display; lenticular liquid crystal display; image super-resolution; antialiasing; multi-view subpixel mapping.

Paper 20210403 received Apr. 15, 2021; accepted for publication Nov. 3, 2021; published online Nov. 23, 2021.

1 Introduction

Visual information is the most important perception of the external world for humans. With the advent of the big data era, the processing of visual information has great potential and significance. Because traditional two-dimensional images can no longer meet people's expectations, the three-dimensional information display technology has emerged at this historic moment and has received extensive attention from the academic community and industry. The naked-eye three-dimensional (3D) image display technology has become a popular research direction in the field of 3D information stereoscopic display because this technology does not need wearing glasses and is convenient and natural.^{1–5} For the naked-eye 3D image display, the synthesis quality of the stereo image directly affects the display quality of the 3D image. Therefore, it is necessary to develop a convenient and effective stereo image synthesis method.

The 3D liquid crystal display system was first proposed by Philips, and the subpixel mapping algorithm proposed by van Berkel is a classical algorithm.⁶ Subsequently, He et al. proposed the general stereoscopic image synthesis method proposed for application to a cylindrical grating with an arbitrary line per inch and an arbitrary tilt angle α . This method can efficiently synthesize and decompose a stereoscopic image with an arbitrary number of viewpoints and an arbitrary resolution.⁷ This method is based on reducing or magnifying each viewpoint image to $1/N$ of the resolution of the composite image (N is the number of viewpoints of the cylindrical grating naked-eye 3D display). The method subsequently maps the pixels corresponding to each viewpoint map based on the subpixel mapping relationship. In composite images, this method suffers from the problem of repeated mapping. Image aliasing occurs when the image is reduced,

*Address all correspondence to Guanglin Yang, ygl@pku.edu.cn

thereby reducing the image-synthesis effect. When the image is enlarged and mapped, the amount of calculation increases.

For spectrum aliasing, Kuang et al.⁸ suggested improving the sampling frequency to eliminate spectral aliasing and achieve better results than those using antialiasing filters. Their proposed method of upsampling using the Scale-2x method has certain advantages compared with the traditional interpolation algorithm. To increase the amount of calculation per unit time after magnifying the image, the viewpoint mask proposed by Cai et al.⁹ can speed up the synthesis speed of the stereogram. Furthermore, it is easy to write to hardware for fast calculation.

Yu et al.¹⁰ proposed a wide-activated deep residual network super-resolution (WDSR) algorithm to reduce parameter quantities and the cost of training by increasing the number of channels of the feature map. Removing redundant convolution layers and network weight normalization improves learning rates and ultimately achieves significantly improved super-resolution. Presently, the WDSR algorithm has better performance than other upsampling algorithms like enhanced deep residual networks for single image super-resolution (ESDR) in many cases. However, nobody had verified its antialiasing performance and effect on the quality of the stereogram composite image so far. Furthermore, the clarity of the stereogram synthesized using the previous upsampling method needs to be improved and better effect of WDSR may help.

In this paper, the WDSR is proposed to optimize the scaling process of images when synthesizing a stereogram. We used a produced mask to accelerate the synthesis process of the stereogram. Compared with traditional interpolation methods applied to stereogram synthesis, the proposed synthesis scheme can reduce image detail loss and eliminate spectral aliasing. It can also improve the signal-to-noise ratio and quality of stereoscopic composite images.

2 Proposed Scheme

As depicted in Fig. 1, the proposed scheme consists mainly of the following four steps.

Step 1: *Zoom in using the WDSR algorithm.* First, we verified its feasibility. We used a DIV2K dataset containing 800 high-definition images. Then 96×96 regions were clipped from each image as the real value. And the images were down sampled from regions clipped as the low-resolution input. After establishing the mapping relationship, the network was trained to achieve the output effect to make the low-resolution map super-resolution. The WDSR-A model, which used the $2\times$ training mode, was adopted.

The DIV2K verification set was used for the effect test. We cropped four images and made the test sets using the bicubic interpolation downsampling method to verify the trained network. Next, we evaluated the super-resolution effect of the algorithm by comparing the peak-signal-to-noise ratio (PSNR) values of WDSR and other methods. We evaluated the antialiasing of the algorithm by comparing the PSNR values of downsampling image after super-resolution using various methods.

If the super-resolution effect and antialiasing of WDSR are better than other methods by comparing the PSNR values (higher PSNR value means better effect), then we zoomed each perspective view to the target stereogram resolution using the WDSR algorithm in combination with the traditional interpolation algorithm since the WDSR algorithm can only achieve integer multiples.

Step 2: *Build a subpixel distribution table.* First, we set up the viewpoint pixel mapping model of our cylindrical grating display (Magnetic 22"Enabl3D) in Fig. 2.

We obtained a subpixel mapping table using the method provided in Ref. 1 (see Fig. 3).

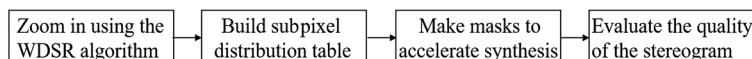
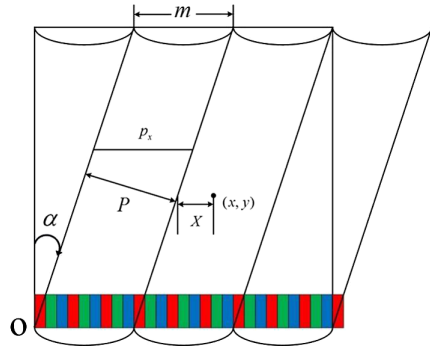


Fig. 1 Optimized stereogram synthesis using WDSR.

**Fig. 2** Viewpoint pixel mapping.

R	G	B	R	G	B	R	G	B	R	G	B	R	G	B			
9	1	2	3	4	5	6	7	8	9	1	2	3	4	5	6	7	8
8	9	1	2	3	4	5	6	7	8	9	1	2	3	4	5	6	7
7	8	9	1	2	3	4	5	6	7	8	9	1	2	3	4	5	6
6	7	8	9	1	2	3	4	5	6	7	8	9	1	2	3	4	5
5	6	7	8	9	1	2	3	4	5	6	7	8	9	1	2	3	4
•	•	•	•	•	•	•	•	•	•	•	•	•	•	•	•	•	•

Fig. 3 Naked-eye 3D display subpixel mapping table.

Step 3: *Make masks to accelerate synthesis.* Based on the method proposed in Ref. 4, we made masks containing 0 and 1 to weigh each perspective view and channel. Finally, we obtained the stereogram. The process is depicted in Fig. 4.

Step 4: *Evaluate stereogram quality.* We calculated the PSNR values of the two stereograms, including the image synthesized in the previous step and that obtained using the traditional method, and judged the quality of the stereogram based on this value. Note that because the quality of WDSR is known to be significantly higher than that of other interpolation algorithms and the target image obtained is closer to the original image, we used the super-resolved image as a reference instead of the original image.

3 Experimental Analysis

The experiments were performed in MATLAB (R2018b), running on a PC with an Intel® Core™ i7-8700 3.20 GHz CPU and a NVIDIA GTX1050Ti GPU.

3.1 Performance Comparison of Image Scaling Algorithms

The DIV2K validation set was used for the effect tests. Four images were cut and down-sampled to create the validation set. The WDSR used the WDSR-A model, and the training mode was magnified twice. The produced high-definition validation dataset is depicted in Fig. 5. The size of each image was $294 \times 294 \times 3$.

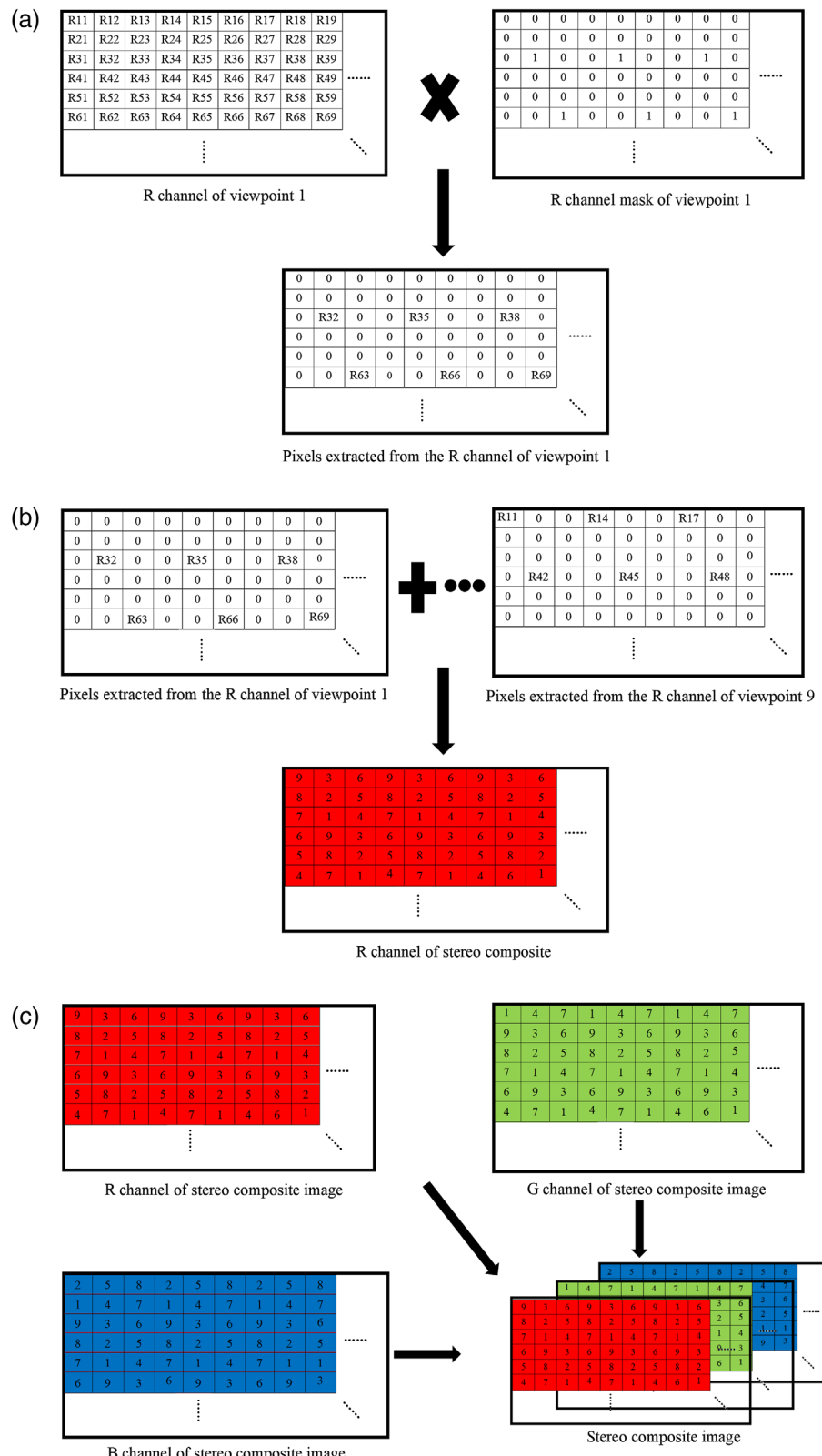


Fig. 4 Process of stereoscopic synthesis: (a) pixels extracted from the R channel of viewpoint 1, (b) R channel of stereo composite image, and (c) process of stereo composite image.

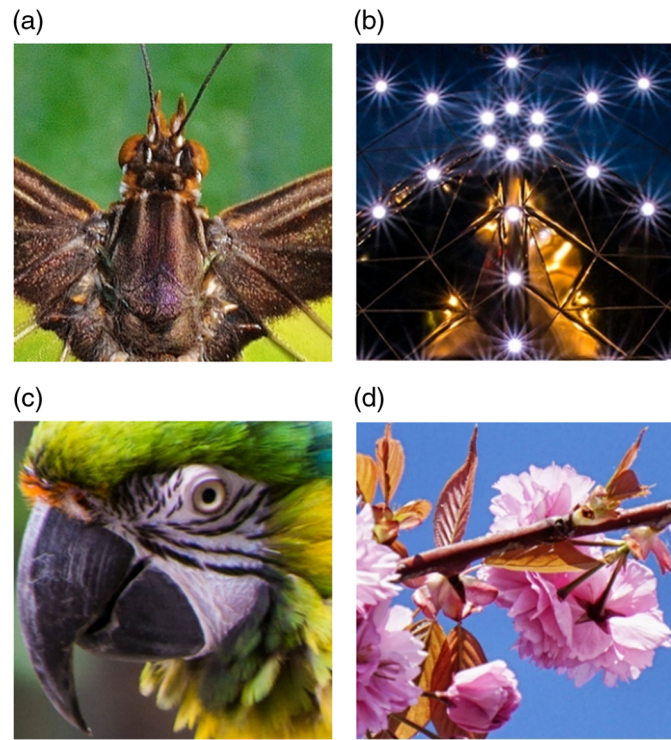


Fig. 5 Test pictures: (a) butterfly, (b) light, (c) parrot, and (d) flower.

The validation process for WDSR was divided into two groups. The first group tested the amplification effects of some scaling algorithms. The size of each image in Fig. 5 was first reduced by a factor of 2 by bicubic interpolation. Next, nearest-neighbor interpolation method, bilinear interpolation method, bicubic interpolation method, Scale-2x algorithm, and WDSR algorithm were separately used to increase the current size of the images by a factor of 2. Finally, we compared the PSNR values of various scaling algorithms (see Table 1).

As is evident from the data in Table 1, the effects of the top three methods improved. Scale-2x had a poor effect on image enlargement. However, WDSR was almost perfect, and its effect was improved significantly compared with those of other scaling algorithms. It retained almost all the information of the original image after image enlargement and was very expressive for the details of the image.

The second was the antialiasing performance test for the original image during downsampling. First, we reduced the size of each image by a factor of 3 indirectly. The size of images in Fig. 5 was first increased by a factor of 2 using the five aforementioned methods and then reduced by a factor of 6 by bicubic interpolation. Next, we compared the PSNR values of the down-sampled images. In other words, the antialiasing performance was tested after the size of original images were reduced by a factor of 3. The results are presented in Table 2.

Table 1 Comparison of the PSNR values of upsampling images using various scaling algorithms.

Scaling algorithm	Butterfly	Light	Parrot	Flower
Nearest neighbor	23.5357	26.2102	30.0454	26.7411
Bilinear	23.5501	26.9611	31.9686	28.1706
Bicubic	24.1100	28.5215	33.7432	29.8920
Scale-2x	19.5140	21.0335	22.9396	20.0524
WDSR	25.3235	34.3802	37.1037	34.6762

Table 2 Comparison of PSNR values of downsampling images using various scaling algorithms (antialiasing).

Scaling algorithm	Butterfly	Light	Parrot	Flower
Nearest neighbor	22.4933	24.8258	29.7471	25.9455
Bilinear	22.4437	24.7052	29.5856	25.7925
Bicubic	22.5102	24.8675	29.8072	26.0007
Scale-2x	22.2730	24.5537	28.8622	25.2267
WDSR	22.5227	24.8953	29.8226	26.0311

From the data in Table 2, the antialiasing optimization function was added to the down-sampling algorithms in MATLAB. Therefore, the results of nearest neighbor (NN), bilinear, and bicubic were beyond the Scale-2x algorithm. It is evident that the WDSR algorithm had a better performance, which was better than the antialiasing optimized function of MATLAB.

3.2 Effect of WDSR Algorithm on the Improvement of Stereoscopic Image Quality

The display quality of the synthesized stereoscopic image was determined mainly from the PSNR value of the image. The image sequences “sugar” and “pat2” in the image dataset captured using the Lytro illum light field camera were used to evaluate the composite effect of the stereogram. The resolution of each image was 382×381 pixels. The basis of comparison was the PSNR value of the stereo composite image obtained through mapping after the image was enlarged using the two methods relative to the original viewpoint. Particularly, the first method of amplification adopted the bicubic interpolation method, which had the best effect in the traditional interpolation method. We considered nine viewpoints of the two sequences (see Fig. 6) and used this method to directly enlarge the original viewpoint image to the viewing resolution of 1024×768 of the display screens. Because it was not an integer multiple, the second method of amplification used a trained WDSR model combined with the traditional interpolation method. First, the size of original viewpoint was enlarged to 1/2 of the required resolution through bicubic interpolation, which had the best effect in traditional scaling methods, that is, 512×384 , (and this resolution was also closer to the original resolution, in which the negative effect of interpolation on image magnification was reduced to the least possible) so that an intermediate

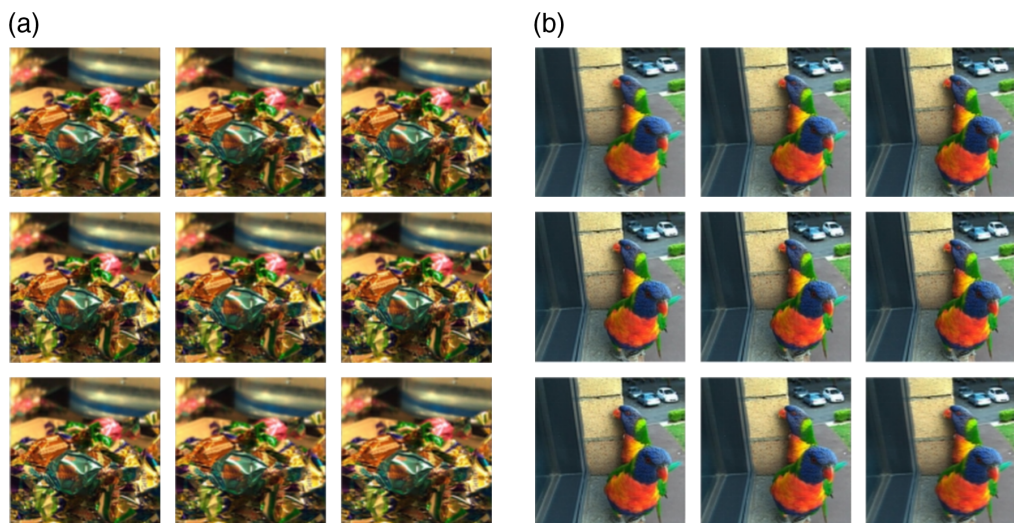
**Fig. 6** Nine viewpoint test image: (a) sugar and (b) pat2.

Table 3 Comparison of PSNR values of sugar stereograms obtained using two scaling methods.

Method	View 1	View 2	View 3	View 4	View 5	View 6	View 7	View 8	View 9
Bicubic	19.49	19.90	20.11	20.23	20.27	20.22	20.08	19.87	19.46
Bicubic + WDSR	19.63	20.04	20.27	20.41	20.45	20.40	20.26	20.03	19.60

Table 4 Comparison of PSNR values of pat2 stereograms obtained using two scaling methods.

Method	View 1	View 2	View 3	View 4	View 5	View 6	View 7	View 8	View 9
Bicubic	22.31	22.70	22.80	22.82	22.79	22.74	22.68	22.33	22.14
Bicubic + WDSR	22.43	22.87	22.99	23.03	23.01	22.98	22.92	22.55	22.31

picture could be obtained. Next, the size of intermediate images was increased by a factor of 2 using the WDSR algorithm, and the to-be-interleaved viewpoints with a resolution of 1024×768 were obtained.

To verify the impact of the above two methods on the effect of the synthesized stereogram, the PSNR values of the two stereograms relative to the original viewpoints were calculated. The quality of the stereogram was determined using this value and actual visual effect. As discussed in the preceding section, the quality of super-resolution by WDSR was significantly higher than that of other interpolation algorithms, and the target image obtained was closer to the original image. Therefore, we used the super-resolved image as a reference image that approximates the original image. We compared the stereograms obtained using the two methods with nine viewpoint images of the two sequences after super-resolution, and Tables 3 and 4 were obtained as follows.

It is evident from the data in tables above that, for all views of sugar and pat2, the PSNR values of the stereograms synthesized using the WDSR algorithm were larger than that synthesized only using bicubic interpolation. More intuitively, we could directly see the

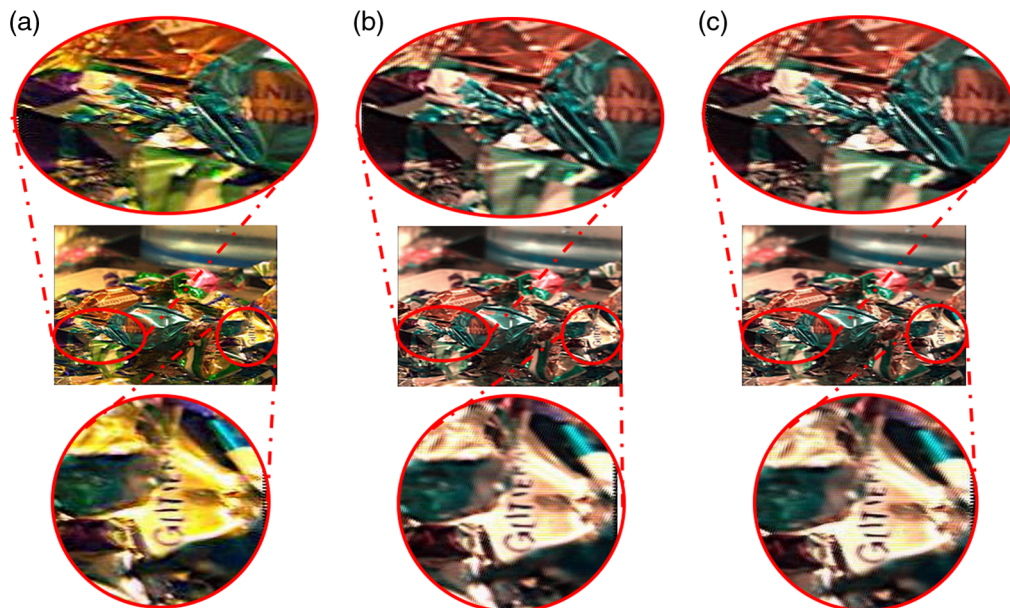


Fig. 7 Comparison between two scaling methods for sugar: (a) viewpoint 1 after WDSR, (b) stereograms synthesized only using bicubic interpolation, and (c) stereograms synthesized using WDSR combined with bicubic interpolation.

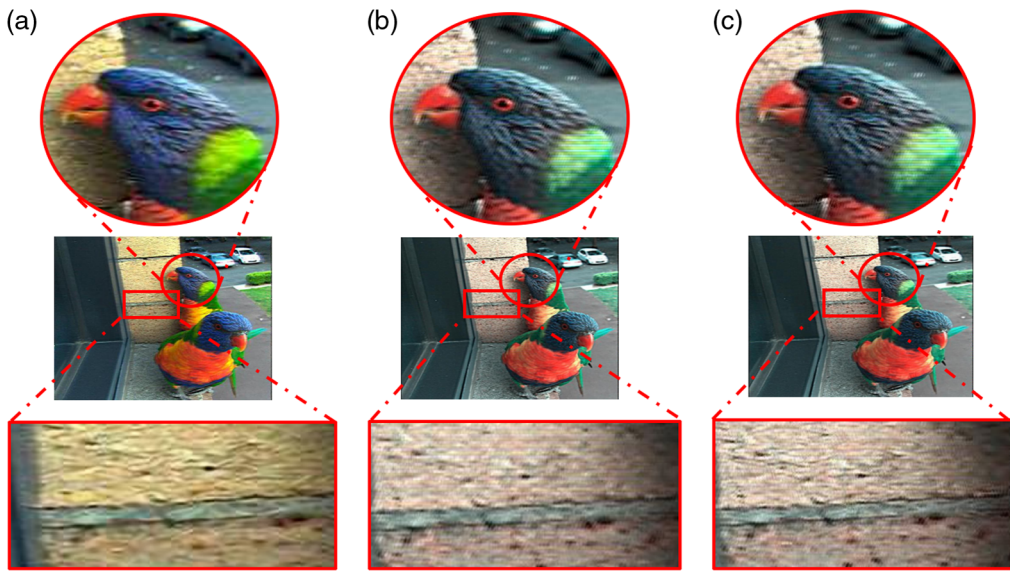


Fig. 8 Comparison between two scaling methods for pat2: (a) viewpoint 1 after WDSR, (b) stereograms synthesized only using bicubic interpolation, and (c) stereograms synthesized using WDSR combined with bicubic interpolation.

improvement from the WDSR algorithm combined with bicubic interpolation through images below (Figs. 7 and 8).

From comparison between stereograms using two scaling methods, the stereograms synthesized using the WDSR algorithm were more clearer than that not using it. Especially in the performance of some details like texture circled above, the stereograms synthesized using the WDSR algorithm were closer to the original images. Unlike only using bicubic interpolation, the WDSR algorithm made stereograms retain more features that have not been smoothed. In addition, in the process of combining traditional algorithms, only one judgment was required, which did not increase the complexity of the algorithm. Moreover, since the WDSR model was pretrained, it could be directly used for amplification. The execution speed would be very fast.

Therefore, the WDSR algorithm actually affected the display quality of the synthesized stereo image. It improved quality of viewing.

4 Conclusion

A multi-view naked-eye three-dimensional image synthesis method based on super-resolution antialiasing is proposed. In this method, the WDSR algorithm is used to optimize the image scaling process and is applied to the traditional synthesis method of multi-view naked-eye 3D images based on cylindrical gratings. The complexity of WDSR is not high, and the execution speed is fast, especially in the case of using GPU. In addition, a mask is used to accelerate the synthesis process of the stereogram. The experimental results show that the proposed scheme can prevent the loss of image detail and spectral aliasing in stereo image synthesis that arises using the traditional interpolation method. It can also improve the signal-to-noise ratio and quality of stereoscopic composite images. The results indicate that this scheme can be applied to the specific application scenarios of multi-view naked-eye 3D image synthesis and display of cylindrical gratings.

Acknowledgments

This research was supported by the Spatial Image Processing Laboratory of Peking University, and the National Science Foundation of China (No. 62071009).

References

1. P. Wang et al., "Computational super-resolution full-parallax three-dimensional light field display based on dual-layer LCD modulation," *IEEE Access* **8**, 81045–81054 (2020).
2. G. J. Lv, B. C. Zhao, and F. Wu, "Real-time viewpoint generation-based 3D display with high-resolution, low-crosstalk, and wide view range," *Opt. Eng.* **59**(10), 103104 (2020).
3. T. Huang et al., "High-performance autostereoscopic display based on the lenticular tracking method," *Opt. Express* **27**(15), 20421–20434 (2019).
4. Z. Yang and G. Yang, "Naked-eye 3D video display using adaptive support-weight algorithm with variable support window," *J. Pattern Recognit. Intell. Syst.* **2**(2) 30–38 (2014).
5. G. Yang, S. Li, and H. Xie, "Naked-eye 3D multi-viewpoint video display," in *Digital Hologr. and 3-D Imaging Meeting*, OSA Technical Digest, paper DTh4A.2, Optical Society of America (2015).
6. C. V. Berkel, "Image preparation for 3D-LCD," *Proc. SPIE* **3639**(2), 84–91 (1999).
7. S.-J. He, "Research on multi-view autostereoscopic display technology based on lenticular grating," Zhejiang University (2009).
8. H.-B. Kuang et al., "Lenticular-based image fusion algorithm for autostereoscopic display," *Comput. Eng.* **37**(3), 207–209 (2011).
9. Y.-F. Cai, "Research on naked eye stereo playback technology," Beijing University of Posts and Telecommunications (2014).
10. J. Yu et al., "Wide activation for efficient and accurate image super-resolution" (2018).

Zheqiang Wang received his BE degree from the Department of Optical Information Science and Technology at Anhui University in July 2016 and his ME degree from the Department of Electronics at the School of Electronics Engineering and Computer Science of Peking University in July 2019. His research interests include image processing and digital holography.

Guanglin Yang received his DE degree from Osaka City University of Japan in 2001 and his ME degree from the Huazhong University of Science and Technology of China in 1993. He is an associate professor at Peking University. He joined Beijing University of Aeronautics and Astronautics of China as a lecturer in 1994. His research interests include optical imaging, digital holography, and image processing. He is a member of IEEE and a senior member of OSA.

Haiyan Xie received her MS and PhD from Osaka City University of Japan in 2002 and 2005, respectively, and her BE and ME degrees from Zhejiang University of China in 1990 and 1992, respectively. She joined Beijing University of Aeronautics and Astronautics of China as a lecturer in 1995. She is a patent attorney at China Science Patent Trademark Agents Ltd. Her research interests include thin film optics and semiconductor materials.